Effect of dimensionality on the optical absorption properties of CsPbI$_3$ perovskite nanocrystals ⊘

Albert Liu; Luiz G. Bonato; Francesco Sessa; Diogo B. Almeida; Erik Isele; Gabriel Nagamine;
Luiz F. Zagonel [ID] ; Ana F. Nogueira [ID] ; Lazaro A. Padilha; Steven T. Cundiff [ID]

Check for updates

🗎 CHORUS

View Online   Export Citation

Articles You May Be Interested In

Fast electron and slow hole spin relaxation in CsPbI$_3$ nanocrystals

Appl. Phys. Lett. (November 2022)

Phase stability investigation of CsPbI$_3$ perovskite for solar cell application

AIP Conf. Proc. (March 2021)

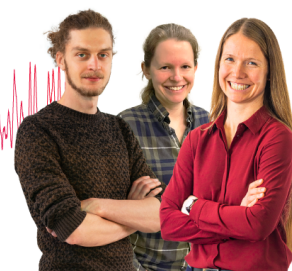Size dependent charge separation and recombination in CsPbI$_3$ perovskite quantum dots

J. Chem. Phys. (August 2019)

The Journal of Chemical Physics

AIP Publishing

Effect of dimensionality on the optical absorption properties of CsPbI₃ perovskite nanocrystals

Albert Liu,[1] Luiz G. Bonato,[2] Francesco Sessa,[1] Diogo B. Almeida,[1,3] Erik Isele,[4] Gabriel Nagamine,[3]
Luiz F. Zagonel,[3] (iD) Ana F. Nogueira,[2] (iD) Lazaro A. Padilha,[3,a)] and Steven T. Cundiff[1,b)] (iD)

AFFILIATIONS

[1] Department of Physics, University of Michigan, Ann Arbor, Michigan 48109, USA
[2] Instituto de Quimica, Universidade Estadual de Campinas, Campinas, Sao Paulo 13083-859, Brazil
[3] Instituto de Fisica, Universidade Estadual de Campinas, Campinas, Sao Paulo 13083-859, Brazil
[4] Department of Electrical Engineering and Computer Science, University of Michigan, Ann Arbor, Michigan 48109, USA

Note: This paper is part of the JCP Special Topic on Colloidal Quantum Dots.
[a)] Electronic mail: padilha@ifi.unicamp.br
[b)] Electronic mail: cundiff@umich.edu

ABSTRACT

The bandgaps of CsPbI₃ perovskite nanocrystals are measured by absorption spectroscopy at cryogenic temperatures. Anomalous bandgap shifts are observed in CsPbI₃ nanocubes and nanoplatelets, which are modeled accurately by bandgap renormalization due to lattice vibrational modes. We find that decreasing dimensionality of the CsPbI₃ lattice in nanoplatelets greatly reduces electron-phonon coupling, and dominant out-of-plane quantum confinement results in a homogeneously broadened absorption line shape down to cryogenic temperatures. An absorption tail forms at low-temperatures in CsPbI₃ nanocubes, which we attribute to shallow defect states positioned near the valence band edge.

*Published under license by AIP Publishing.* https://doi.org/10.1063/1.5124399

I. INTRODUCTION

Colloidal nanocrystals, following decades of extensive study, have begun maturing as a material platform for commercial applications such as displays[1] and photovoltaics.[2] However, despite more than 30 years of research into alternative material platforms, the initial chalcogenide-based colloidal nanocrystals have remained superior in both performance and stability for practical devices. Recently, synthesis of cesium lead-halide perovskite nanocrystals has been achieved,[3] which has generated much excitement due to their exceptional optical properties.

Shortly following the initial synthesis of perovskite nanocubes (NCs), synthesis of perovskite nanoplatelets (NPs)[4,5] was also achieved to further broaden the gamut of applications for perovskite nanocrystals. Compared to their nanocube counterparts, the nanoplatelet geometry offers directional light absorption/emission[6] as well as reduced dielectric screening (leading to greatly enhanced exciton binding energies[7] and radiative recombination

rates[8,9]). Recently, these attractive properties have led to intense efforts in applying perovskite nanoplatelets toward a variety of applications such as light-emitting diodes[10] and photovoltaics.[11] Understanding how electronic dynamics underlying the photophysics of perovskite nanocrystals change with the nanocrystal geometry is crucial for such practical applications. In particular, perovskite nanoplatelets have been seldom studied at cryogenic temperature to elucidate electron-phonon coupling in the material.

Here, we study CsPbI₃ perovskite nanocube and nanoplatelet ensembles at cryogenic temperatures. Absorption spectra reveal an anomalous bandgap shift to higher energies with increasing temperature, which we attribute to bandgap renormalization via electron-phonon coupling. A low-energy absorption tail is also observed in CsPbI₃ nanocubes that is likely due to shallow trap states, which implies that iodide perovskite nanocrystals may be less defect-tolerant than their bromide and chloride counterparts at low temperatures.
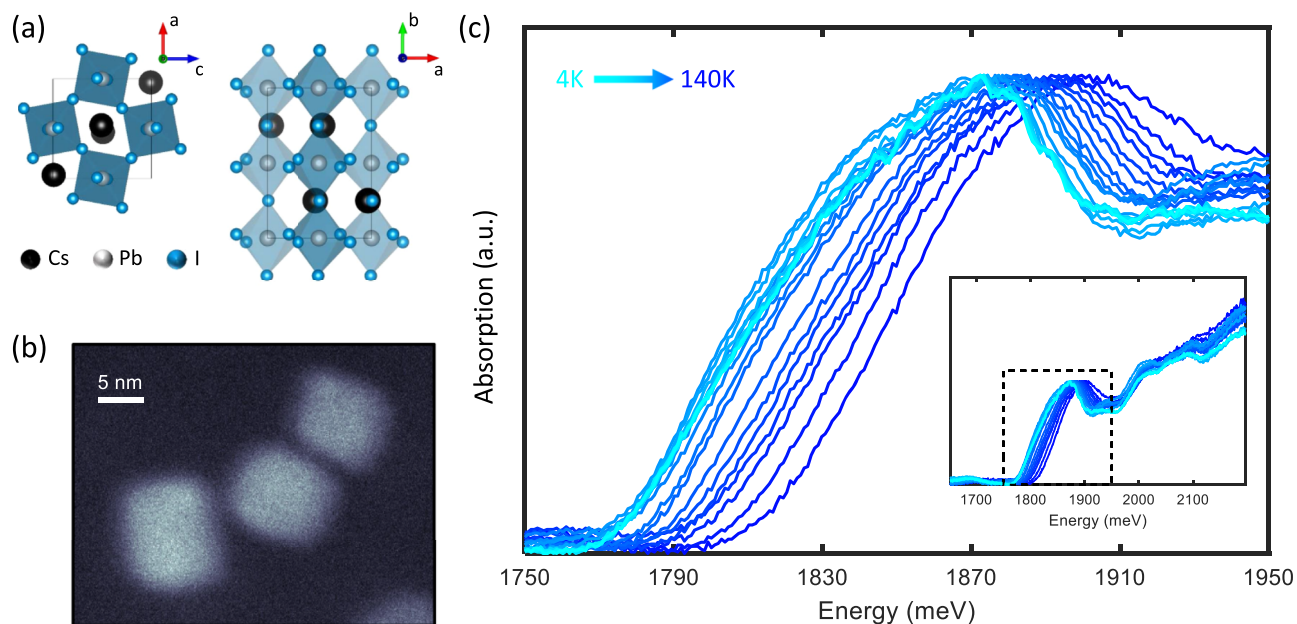
FIG. 1. (a) Two perspective views of the orthorhombic perovskite lattice structure of CsPbI$_3$ with axes as shown (plotted using the VESTA software[18]). The unit cell is denoted by the solid black lines. (b) Transmission electron micrograph of nanocubes. (c) Absorption spectra of CsPbI$_3$ nanocrystals at temperatures ranging from 4 K to 140 K as indicated. The full-range spectra are plotted in the inset, while the 1S exciton peak outlined by the dashed box is shown in the main plot. The specific temperatures plotted are indicated by the data in Fig. 2(b).

II. EXPERIMENT

The orthorhombic perovskite lattice structure of the CsPbI$_3$ nanocrystals[12–14] is shown in Fig. 1(a), and transmission electron micrographs of the nanocubes are shown in Fig. 1(b). The measurement of 100 nanocubes reveals an average side length of 8.7 ± 2.6 nm. Although significant size and shape dispersion of the nanoplatelets preclude well-defined average side lengths, their lateral dimensions are on the order of tens of nanometers (see the supplementary material). Their bandgap energy then indicates the out-of-plane thickness to be primarily four polyhedral layers and above.

The nanocubes are synthesized according to the procedures detailed by Protesescu et al.,[3,15] and the nanoplatelets are synthesized via a method[16] modified from that reported by Sheng et al.[17] Brief descriptions of each method are detailed in the supplementary material.

To study their optical properties at cryogenic temperatures, we redisperse the nanocrystals in heptamethylnonane, a branched alkane that forms a transparent glass at cryogenic temperatures.[19] The colloidal suspension is held in a custom sample holder approximately 0.5 mm thick and mounted on a cold-finger cryostat. Absorption spectra are measured with a broadband white light source and a UV-vis diode array spectrometer.

III. RESULTS AND DISCUSSION

CsPbI$_3$ nanocube absorption spectra normalized to the lowest-energy 1S exciton absorption peak at temperatures ranging from 4 K to 140 K are plotted in Fig. 1(c). Although multiple peaks are observed that correspond to distinct exciton transitions, here we focus on the 1S exciton absorption peak that reflects the fundamental electronic bandgap (energy-gap) of the nanocrystals. As temperature increases, the bandgap exhibits a pronounced blue shift to higher energies, which is contrary to the red shift observed in most solids. In the literature, this phenomenon has been referred to as an anomalous bandgap shift.[20–23]

To quantify the bandgap shift, we fit the peaks with Gaussian line shapes that reflect the size distribution of the nanocrystals. As shown in Fig. 2(a), we fit only the top of each peak due to absorption tails present at lower temperatures. The widths σ of each Gaussian fit, allowed to vary freely, do not change significantly with temperature (mean width 41.81 meV and standard deviation 3.37 meV). The fitted Gaussian center energies (which agree closely with center energies found from a fourth-order polynomial fit) are plotted in Fig. 2(b), which reveals interesting behavior at temperatures below 50 K. Specifically, two clear inflection points at 20 and 30 K are observed that reveal more complicated bandgap behavior than previously reported for photoluminescence measurements of similar perovskite nanocubes.[23]

The dependence of the electronic bandgap on temperature T may be expressed as[22,24]

$$E_g(T) = E_0 + AT + \sum_n B_n \left(\frac{1}{e^{\hbar\omega_n/k_B T} - 1} + \frac{1}{2} \right). \quad (1)$$

The first term E_0 is the intrinsic material bandgap at $T = 0$, and the coefficient A in the second term characterizes the change in the bandgap due to lattice unit cell expansion/contraction (in the
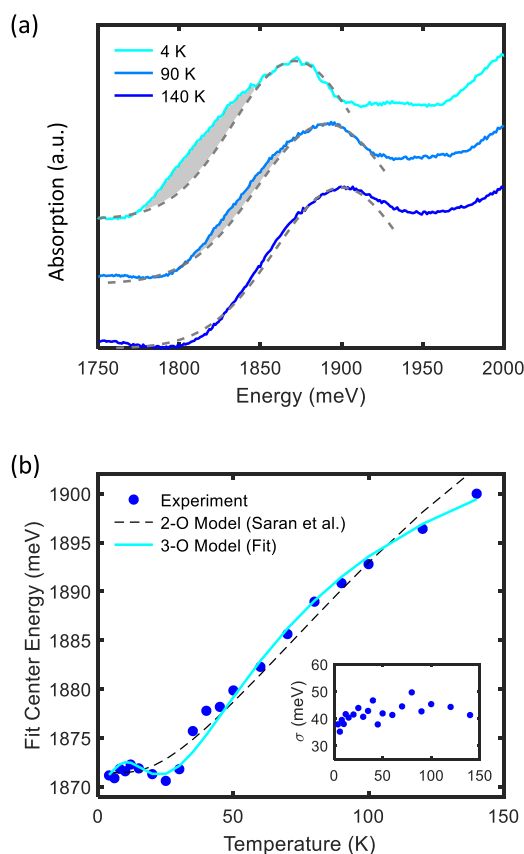
FIG. 2. (a) Gaussian peak fits of CsPbI$_3$ absorption spectra at three representative temperatures, 4, 90, and 140 K. A low-energy absorption tail, indicated by the shaded gray region, forms at low temperature. (b) Dark-blue dots show fitted Gaussian center energy as a function of temperature, which reflects the material bandgap. A two-oscillator (2-O) model using the fitted parameters from Saran *et al.*[23] and a fit to the three-oscillator (3-O) model described in the text are then plotted as the dashed black curve and the solid light-blue curve, respectively. The fitted Gaussian widths σ are plotted in the inset.

so-called quasiharmonic approximation[24]). Here, the change in quantum confinement energy due to the expansion/contraction of the nanocrystal volume, which we expect to be negligible at low temperatures,[25] is ignored. The third term then represents renormalization of the bandgap due to electron-phonon interactions, where n is summed over all phonon branches and all wave-vectors within the Brillouin zone for each branch. B_n and $\hbar\omega_n$ are the electron-phonon coupling strength and vibrational energy, respectively, for mode n. Whether B_n is positive or negative, resulting in an increase or decrease of the bandgap, respectively, arises from a complex interplay of microscopic dynamics and cannot be predicted easily from the properties of a given phonon branch.[20,26] However, accounting for all possible phonon branches throughout the Brillouin zone is often unnecessary in modeling the behavior of real systems. Instead, one[27] or two[20] vibrational modes are usually assumed dominant (referred to as one-oscillator and two-oscillator models), which reduces the summation to either one or two terms, respectively.

Here, we find both the one-oscillator and two-oscillator models to be insufficient in modeling the bandgap temperature dependence observed for CsPbI$_3$ nanocubes. As mentioned above, two inflection points are observed that necessitate at least three dominant vibrational modes that independently renormalize the bandgap. A least-squares fit of the bandgap temperature dependence to this three-oscillator model is plotted in Fig. 2(b), where good agreement is observed at both high and low temperatures. The fitted parameters are E_0 = 1916.9 meV, A = 0.3 meV/K, $\hbar\omega_1$ = 5.38 meV, $\hbar\omega_2$ = 5.91 meV, $\hbar\omega_3$ = 17.02 meV, B_1 = −698.01 meV, B_2 = 821.67 meV, and B_3 = −217.39 meV. Instead of the acoustic and optical phonon categories that are usually invoked for two-oscillator models,[22,23] a three-oscillator model in perovskite materials align more naturally to the bending, stretching, and rocking perovskite vibrational modes that possess distinct ranges of vibrational energies.[28]

We note that although the two-oscillator model was recently invoked by Saran *et al.* to model the temperature dependence of photoluminescence center energy in perovskite nanocrystals,[23] the data points taken at low temperatures (below 50 K) were too sparse to resolve the two inflection points we observe. Their resultant fitted bandgap dependence is plotted in Fig. 2(b) for comparison. In contrast to features in absorption spectra, which are simply proportional to the oscillator strength of each optical transition, features in photoluminescence spectra depend on many other temperature-dependent factors such as the equilibrium fine-structure carrier distribution[29,30] and emission Stokes shifts.[31] It is therefore unclear whether the apparent two-oscillator behavior of their measurements on CsPbI$_3$ nanocubes was due to coarse-graining effects or the above confounding factors in temperature-dependent photoluminescence.

Lower-energy absorption tails are observed. For ideal nanocubes, the exciton density of states are comprised of delta functions that result in roughly Gaussian absorption peaks (reflecting the nanocrystal size distribution). Absorption tails at lower-energy are therefore indicative of corresponding tails of the electronic density of states, often attributed to impurities[32] or surface states.[33] As shown in Fig. 2(a), the absorption peak is Gaussian at 140 K and develops a lower-energy tail with decreasing temperature. We attribute this tail to shallow defect states surrounding the valence band edge that have been shown to arise from lattice point defects.[34] At high temperatures, valence band electrons populate the band edge in a thermal equilibrium distribution. At low temperatures, those electrons then fill the defect states from lowest energy upward, which comprise a Halperin-Lax type distribution[35] with a $\exp(\sqrt{E})$ dependence.[36,37] The disappearance of the tail at 140 K thus suggests a few millielectronvolts (comparable to the 140 K Boltzmann energy of 12 meV) defect state energy distribution. Although, in principle, such defect state absorption should manifest in photoluminescence spectra as well, no clear band-tailing was observed in low-temperature photoluminescence measurements.[23] This is unsurprising since above-gap excitation results in competing band edge and defect state relaxation pathways and emission Stokes shifts (on the order of tens of millielectronvolts in perovskite nanocrystals[3,23]) likely differ for defect transitions. For additional comparison, absorption measurements were also performed on CsPbBr$_3$ nanocubes (see the supplementary material for absorption spectra and synthesis methods). Although a large anomalous bandgap

shift was observed (approximately 40 meV from 6 to 140 K), no absorption tail forms at low temperatures.

Electron-phonon coupling that renormalizes the $CsPbI_3$ bandgap should depend strongly on dimensionality in nanocrystals. In particular, lowering dimensionality should reduce electron-phonon coupling by restricting certain vibrational modes. To investigate the effect of lattice dimensionality on electron-phonon
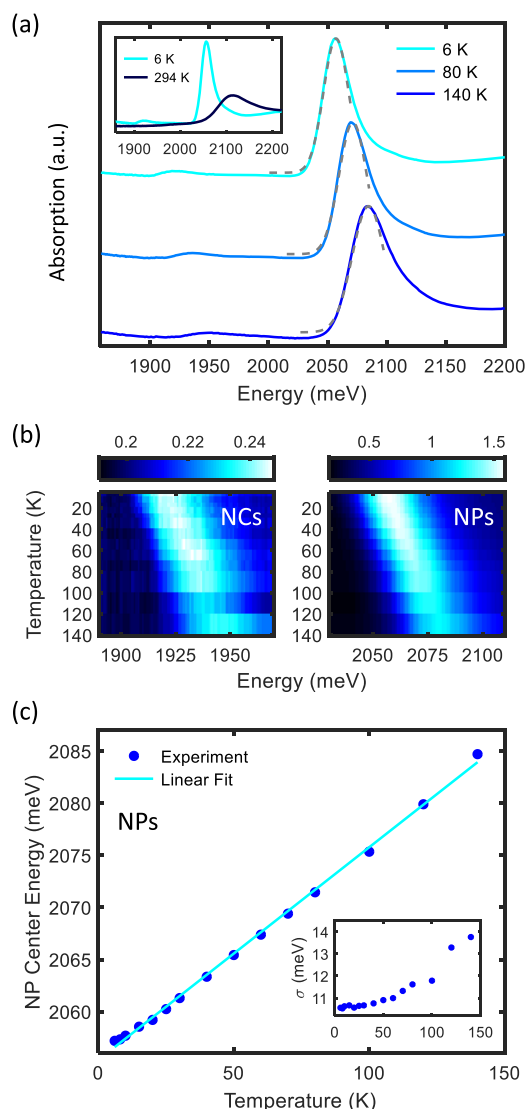
FIG. 3. (a) Absorption spectra of $CsPbI_3$ nanoplatelets at three representative temperatures, 6, 80, and 140 K. In addition to the main nanoplatelet (NP) absorption peak, a weak nanocube (NC) absorption peak at lower energy appears at low temperatures. The inset shows comparison between 6 K and room-temperature absorption spectra. (b) Optical density surface plots of the NC and NP absorption peaks in (a) as a function of temperature. (c) NP center energies obtained from the absorption peak first moment as a function of temperature, which reflects the material bandgap. A linear fit is plotted as the solid blue curve. The fitted Gaussian widths are plotted in the inset, which monotonically decrease with decreasing temperature.

coupling, we repeat the same temperature-dependent absorption measurements on $CsPbI_3$ nanoplatelets. At room-temperature, a single nanoplatelet absorption peak is observed that is blue shifted relative to the nanocube bandgap due to strong quantum confinement in the out-of-plane direction. At cryogenic temperatures, shown in Fig. 3, the absorption spectrum changes in two surprising ways. First, the nanoplatelet absorption peak continues narrowing below 140 K (with no absorption tail), in contrast to the nanocube absorption peak width that remains constant at low temperatures. Second, an additional lower-energy peak also appears with decreasing temperature [see Fig. 3(a)], which, due to its center energy, we attribute to cosynthesized $CsPbI_3$ nanocubes. Temperature-dependent surface plots of both the nanocube and nanoplatelet peaks (measured from the same absorption spectra) are shown in Fig. 3(b), demonstrating the relative changes in peak optical density.

Again the nanoplatelet absorption peaks are fitted to the Gaussian line shapes, and the fitted center energies are plotted in Fig. 3(c). The nearly linear anomalous bandgap shift indicates weakened electron-phonon interactions and greater importance of bandgap renormalization due to unit cell expansion/contraction with temperature. To quantify these changes, we perform a linear fit of the center energy temperature-dependence. The fitted parameters are $E_0 = 2055.4$ meV and $A = 0.2$ meV/K, where A is comparable to its corresponding nanocube value. Therefore, decreasing dimensionality greatly reduces vibrational bandgap renormalization without strongly affecting that due to changes in unit cell size.

The fitted Gaussian widths σ, plotted in the inset in Fig. 3(c), reveal another interesting aspect of the electronic properties of perovskite nanoplatelets. While the nanocube absorption peak width is approximately constant at cryogenic temperatures, reflecting its inhomogeneously broadened nature, the much narrower nanoplatelet absorption peak exhibits a monotonic decrease in σ with decreasing temperature. This indicates that homogeneous broadening in perovskite nanoplatelets contributes even down to cryogenic temperatures. However, a plateau in the linewidth that decreases below 50 K, despite homogeneous out-of-plane confinement, reveals an intrinsic ensemble absorption linewidth between 10 and 11 meV. At such energy scales, inhomogeneous broadening due to variation in the in-plane confinement of exciton center-of-mass motion, usually considered to be negligible,[38] could become important. More advanced spectroscopic techniques such as multidimensional coherent spectroscopy[39] are needed to disentangle inhomogeneous and homogeneous broadening mechanisms in perovskite nanoplatelets.[19,40]

IV. CONCLUSION

In summary, the absorption of $CsPbI_3$ perovskite nanocrystals is measured at cryogenic temperatures. In conjunction with the anomalous bandgap shifts to higher energies with increasing temperature, additional inflection points are observed at low temperatures; which we attribute to bandgap renormalization by three vibrational modes in $CsPbI_3$ nanocubes, contrary to a recent study.[23] The measurement of $CsPbI_3$ nanoplatelets then reveals greatly reduced vibrational bandgap renormalization, which suggests that lowered nanocrystal dimensionality leads to weakened influence of lattice vibrations on electronic dynamics. Finally, absorption tails are

found to form in $CsPbI_3$ nanocubes at low temperatures, which we attribute to defect states surrounding the valence band edge. While perovskite nanocrystals have been found to be exceptionally defect-tolerant,[41] our finding suggests that shallow defects may begin to influence the optical properties of iodide nanocubes at cryogenic temperatures. This work motivates further study of electron-phonon coupling in perovskite nanocrystals to minimize their deleterious effects.

SUPPLEMENTARY MATERIAL

In the supplementary material, we provide details of the nanocrystal synthesis procedures, absorption temperature dependences of $CsPbBr_3$ nanocubes, and supplemental TEM images of the iodide nanoplatelets and bromide nanocubes.

ACKNOWLEDGMENTS

REFERENCES

[1]M. K. Choi, J. Yang, T. Hyeon, and D.-H. Kim, "Flexible quantum dot light-emitting diodes for next-generation displays," npj Flexible Electron. **2**, 10 (2018).

[2]M. Yuan, M. Liu, and E. H. Sargent, "Colloidal quantum dot solids for solution-processed solar cells," Nat. Energy **1**, 16016 (2016).

[3]L. Protesescu, S. Yakunin, M. I. Bodnarchuk, F. Krieg, R. Caputo, C. H. Hendon, R. X. Yang, A. Walsh, and M. V. Kovalenko, "Nanocrystals of cesium lead halide perovskites ($CsPbX_3$, X = Cl, Br, and I): Novel optoelectronic materials showing bright emission with wide color gamut," Nano Lett. **15**, 3692–3696 (2015).

[4]Y. Bekenstein, B. A. Koscher, S. W. Eaton, P. Yang, and A. P. Alivisatos, "Highly luminescent colloidal nanoplates of perovskite cesium lead halide and their oriented assemblies," J. Am. Chem. Soc. **137**, 16008–16011 (2015).

[5]Y. Tong, E. Bladt, M. F. Aygüler, A. Manzi, K. Z. Milowska, V. A. Hintermayr, P. Docampo, S. Bals, A. S. Urban, L. Polavarapu, and J. Feldmann, "Highly luminescent cesium lead halide perovskite nanocrystals with tunable composition and thickness by ultrasonication," Angew. Chem., Int. Ed. **55**, 13887–13892 (2016).

[6]M. J. Jurow, T. Morgenstern, C. Eisler, J. Kang, E. Penzo, M. Do, M. Engelmayer, W. T. Osowiecki, Y. Bekenstein, C. Tassone, L.-W. Wang, A. P. Alivisatos, W. Brütting, and Y. Liu, "Manipulating the transition dipole moment of $CsPbBr_3$ perovskite nanocrystals for superior optical properties," Nano Lett. **19**, 2489–2496 (2019).

[7]Q. Wang, X.-D. Liu, Y.-H. Qiu, K. Chen, L. Zhou, and Q.-Q. Wang, "Quantum confinement effect and exciton binding energy of layered perovskite nanoplatelets," AIP Adv. **8**, 025108 (2018).

[8]V. A. Hintermayr, A. F. Richter, F. Ehrat, M. Döblinger, W. Vanderlinden, J. A. Sichert, Y. Tong, L. Polavarapu, J. Feldmann, and A. S. Urban, "Tuning the optical properties of perovskite nanoplatelets through composition and thickness by ligand-assisted exfoliation," Adv. Mater. **28**, 9478–9485 (2016).

[9]M. C. Weidman, A. J. Goodman, and W. A. Tisdale, "Colloidal halide perovskite nanoplatelets: An exciting new class of semiconductor nanomaterials," Chem. Mater. **29**, 5019–5030 (2017).

[10]S. Peng, S. Wang, D. Zhao, X. Li, C. Liang, J. Xia, T. Zhang, G. Xing, and Z. Tang, "Pure bromide-based perovskite nanoplatelets for blue light-emitting diodes," Small Methods **3**, 1900196 (2019).

[11]M. Wei, F. P. G. de Arquer, G. Walters, Z. Yang, L. N. Quan, Y. Kim, R. Sabatini, R. Quintero-Bermudez, L. Gao, J. Z. Fan, F. Fan, A. Gold-Parker, M. F. Toney, and E. H. Sargent, "Ultrafast narrowband exciton routing within layered perovskite nanoplatelets enables low-loss luminescent solar concentrators," Nat. Energy **4**, 197–205 (2019).

[12]P. Cottingham and R. L. Brutchey, "On the crystal structure of colloidally prepared $CsPbBr_3$ quantum dots," Chem. Commun. **52**, 5246–5249 (2016).

[13]F. Bertolotti, L. Protesescu, M. V. Kovalenko, S. Yakunin, A. Cervellino, S. J. L. Billinge, M. W. Terban, J. S. Pedersen, N. Masciocchi, and A. Guagliardi, "Coherent nanotwins and dynamic disorder in cesium lead halide perovskite nanocrystals," ACS Nano **11**, 3819–3831 (2017).

[14]R. J. Sutton, M. R. Filip, A. A. Haghighirad, N. Sakai, B. Wenger, F. Giustino, and H. J. Snaith, "Cubic or orthorhombic?: Revealing the crystal structure of metastable black-phase $CsPbI_3$ by theory and experiment," ACS Energy Lett. **3**, 1787–1794 (2018).

[15]L. Protesescu, S. Yakunin, S. Kumar, J. Bär, F. Bertolotti, N. Masciocchi, A. Guagliardi, M. Grotevent, I. Shorubalko, M. I. Bodnarchuk, C.-J. Shih, and M. V. Kovalenko, "Dismantling the "red wall" of colloidal perovskites: Highly luminescent formamidinium and formamidinium-cesium lead iodide nanocrystals," ACS Nano **11**, 3119–3134 (2017).

[16]L. G. Bonato, R. F. Moral, G. Nagamine, A. A. de Oliveira, J. C. Germino, D. S. da Silva, F. Galembeck, L. A. Padilha, and A. F. Nogueira, "Revealing the role of tin (IV) halides in the anisotropic growth of $CsPbX_3$ perovskite nanoplates" (unpublished).

[17]X. Sheng, G. Chen, C. Wang, W. Wang, J. Hui, Q. Zhang, K. Yu, W. Wei, M. Yi, M. Zhang, Y. Deng, P. Wang, X. Xu, Z. Dai, J. Bao, and X. Wang, "Polarized opto-electronics of $CsPbX_3$ (X = Cl, Br, I) perovskite nanoplates with tunable size and thickness," Adv. Funct. Mater. **28**, 1800283 (2018).

[18]K. Momma and F. Izumi, "*VESTA3* for three-dimensional visualization of crystal, volumetric and morphology data," J. Appl. Crystallogr. **44**, 1272–1276 (2011).

[19]A. Liu, D. B. Almeida, W. K. Bae, L. A. Padilha, and S. T. Cundiff, "Non-Markovian exciton-phonon interactions in core-shell colloidal quantum dots at femtosecond timescales," Phys. Rev. Lett. **123**, 057403 (2019).

[20]A. Göbel, T. Ruf, M. Cardona, C. T. Lin, J. Wrzesinski, M. Steube, K. Reimann, J.-C. Merle, and M. Joucla, "Effects of the isotopic composition on the fundamental gap of CuCl," Phys. Rev. B **57**, 15183–15190 (1998).

[21]I.-H. Choi and P. Y. Yu, "Suppression of the anomalous blue shift in the band gap temperature dependence of $AgCuGaS_2$ alloys," Phys. Rev. B **63**, 235210 (2001).

[22]C. Yu, Z. Chen, J. J. Wang, W. Pfenninger, N. Vockic, J. T. Kenney, and K. Shum, "Temperature dependence of the band gap of perovskite semiconductor compound $CsSnI_3$," J. Appl. Phys. **110**, 063526 (2011).

[23]R. Saran, A. Heuer-Jungemann, A. G. Kanaras, and R. J. Curry, "Giant bandgap renormalization and exciton-phonon scattering in perovskite nanocrystals," Adv. Opt. Mater. **5**, 1700231 (2017).

[24]M. Cardona, "Electron-phonon interaction in tetrahedral semiconductors," Solid State Commun. **133**, 3–18 (2005).

[25]N. M. Badlyan, A. Biermann, T. Aubert, Z. Hens, and J. Maultzsch, "Thermal expansion of colloidal CdSe/CdS core/shell quantum dots," Phys. Rev. B **99**, 195425 (2019).

[26]N. Garro, A. Cantarero, M. Cardona, A. Göbel, T. Ruf, and K. Eberl, "Dependence of the lattice parameters and the energy gap of zinc-blende-type semiconductors on isotopic masses," Phys. Rev. B **54**, 4732–4740 (1996).

[27]I.-H. Choi, S.-H. Eom, and P. Y. Yu, "Soft phonon mode and the anomalous temperature dependence of band gap in $AgGaS_2$," Phys. Status Solidi B **215**, 99–104 (1999).

[28]M. A. Pérez-Osorio, R. L. Milot, M. R. Filip, J. B. Patel, L. M. Herz, M. B. Johnston, and F. Giustino, "Vibrational properties of the organic-inorganic halide perovskite $CH_3NH_3PbI_3$ from theory and experiment: Factor group analysis, first-principles calculations, and low-temperature infrared spectra," J. Phys. Chem. C **119**, 25703–25718 (2015).

[29]C. Yin, L. Chen, N. Song, F. Lv, F. Hu, C. Sun, W. W. Yu, C. Zhang, X. Wang, Y. Zhang, and M. Xiao, "Bright-exciton fine-structure splittings in single perovskite nanocrystals," Phys. Rev. Lett. **119**, 026401 (2017).

[30]G. Raino, G. Nedelcu, L. Protesescu, M. I. Bodnarchuk, M. V. Kovalenko, R. F. Mahrt, and T. Stoferle, "Single cesium lead halide perovskite nanocrystals

at low temperature: Fast single-photon emission, reduced blinking, and exciton fine structure," ACS Nano **10**, 2485–2490 (2016).

[31] H. Qiao, K. A. Abel, F. C. J. M. van Veggel, and J. F. Young, "Exciton thermalization and state broadening contributions to the photoluminescence of colloidal PbSe quantum dot films from 295 to 4.5 K," Phys. Rev. B **82**, 165435 (2010).

[32] I. Studenyak, M. Kranjec, and M. Kurik, "Urbach rule in solid state physics," Int. J. Opt. Appl. **4**, 76–83 (2014).

[33] P. Guyot-Sionnest, E. Lhuillier, and H. Liu, "A mirage study of CdSe colloidal quantum dot films, urbach tail, and surface states," J. Chem. Phys. **137**, 154704 (2012).

[34] J. Kang and L.-W. Wang, "High defect tolerance in lead halide perovskite CsPbBr$_3$," J. Phys. Chem. Lett. **8**, 489–493 (2017).

[35] B. I. Halperin and M. Lax, "Impurity-band tails in the high-density limit. I. Minimum counting methods," Phys. Rev. **148**, 722–740 (1966).

[36] R. Yan, W. Zhang, W. Wu, X. Dong, Q. Wang, and J. Fan, "Optical spectroscopy reveals transition of CuInS$_2$/ZnS to Cu$_x$Zn$_{1-x}$InS$_2$/ZnS:Cu alloyed quantum dots with resultant double-defect luminescence," APL Mater. **4**, 126101 (2016).

[37] J. Jean, T. S. Mahony, D. Bozyigit, M. Sponseller, J. Holovský, M. G. Bawendi, and V. Bulovic, "Radiative efficiency limit with band tailing exceeds 30% for quantum dot solar cells," ACS Energy Lett. **2**, 2616–2624 (2017).

[38] M. Nasilowski, B. Mahler, E. Lhuillier, S. Ithurria, and B. Dubertret, "Two-dimensional colloidal nanocrystals," Chem. Rev. **116**, 10934–10982 (2016).

[39] S. T. Cundiff and S. Mukamel, "Optical multidimensional coherent spectroscopy," Phys. Today **66**(7), 44–49 (2013).

[40] A. Liu, D. B. Almeida, W.-K. Bae, L. A. Padilha, and S. T. Cundiff, "Simultaneous existence of confined and delocalized vibrational modes in colloidal quantum dots," J. Phys. Chem. Lett. **10**, 6144–6150 (2019).

[41] H. Huang, M. I. Bodnarchuk, S. V. Kershaw, M. V. Kovalenko, and A. L. Rogach, "Lead halide perovskite nanocrystals in the research spotlight: Stability and defect tolerance," ACS Energy Lett. **2**, 2071–2083 (2017).

23 September 2025 19:27:24